

Sharply increasing effective mass: a precursor of the spontaneous spin polarization in a dilute two-dimensional electron system

A. A. Shashkin^{y,z}, S. V. Kravchenko^y, V. T. Dolgoplov^z and T. M. Klapwijk^k

^y Physics Department, Northeastern University, Boston, MA 02115, U.S.A.

^z Institute of Solid State Physics, Chernogolovka, Moscow District 142432, Russia

^k Department of Applied Physics, Delft University of Technology, 2628 C.J.D. elft, The Netherlands

Abstract. We have measured the effective mass, m^* , and Lande g factor in very dilute two-dimensional electron systems in silicon. Two independent methods have been used: (i) analysis of the Shubnikov-de Haas oscillations and (ii) measurements of the magnetic field required to fully polarize the electrons' spins. We have observed a sharp increase of the effective mass with decreasing electron density while the g factor remains nearly constant and close to its value in bulk silicon. The corresponding strong rise of the spin susceptibility $\chi_{\text{spin}} / g m^*$ may be a precursor of a spontaneous spin polarization; unlike in the Stoner scenario, it originates from the enhancement of the effective mass rather than from the increase of g factor. Furthermore, using tilted magnetic fields, we have found that the enhanced effective mass is independent of the degree of spin polarization and, therefore, its increase is not related to spin exchange effects, in contradiction with existing theories. Our results show that the dilute 2D electron system in silicon behaves well beyond a weakly interacting Fermi liquid.

PACS numbers: 71.30.+h, 73.40.Qv, 71.18.+y

E-mail: s.kravchenko@neu.edu

1. Introduction

At sufficiently low electron densities, two-dimensional (2D) electron systems become strongly correlated, because the kinetic energy is overpowered by energy of electron-electron interactions. The strength of the interactions is usually characterized by the ratio between the Coulomb energy and the Fermi energy, $r_s = E_c/E_F$, which, assuming that the effective electron mass is equal to the band mass, in the system with single-valley spectrum reduces to the Wigner-Seitz radius, $l = (n_s)^{-1/2} a_B$ (here n_s is the electron density and a_B is the Bohr radius in semiconductor). There are several suggested candidates for the ground state of the system, for example, (i) Wigner crystal characterized by spatial and spin ordering [1], (ii) ferromagnetic Fermi liquid with spontaneous spin ordering [2], and (iii) paramagnetic Fermi liquid [3]. In the strongly-interacting limit ($r_s \gg 1$), no analytical theory has been developed to date.

To whom correspondence should be addressed

According to numeric simulations [4], Wigner crystallization is expected in a very dilute regime, when r_s reaches approximately 35. The recent numeric simulations [5] have predicted that prior to the crystallization, in the range of the interaction parameter $25 < r_s < 35$, the ground state of the system is a strongly correlated ferromagnetic Fermi liquid. A paramagnetic Fermi liquid is realized at yet higher electron densities when the interactions are relatively weak ($r_s \approx 1$). The effective mass, m^* , and Lande g factor within the Fermi liquid theory are renormalized due to spin exchange effects, with renormalization of the g factor being dominant compared to that of the effective mass [6]. Alternatively, near the onset of Wigner crystallization, strong increase of the effective mass is expected [7, 8].

Recently, there has been a lot of interest in the electron properties of dilute 2D systems due to the observation of an unexpected metal-insulator transition (MIT) in zero magnetic field, strong metallic temperature dependence of the resistance in these systems, and a giant positive magnetoresistance in a magnetic field parallel to the 2D plane (for a review, see Ref. [9]). The most pronounced effects have been observed in high-mobility silicon metal-oxide-semiconductor field-effect transistors (MOSFETs), with the low-temperature drop of the resistance reaching an order of magnitude and magnetoresistance exceeding several orders of magnitude. Significant progress has been recently made in understanding the metallic behaviour of the resistivity and its suppression by a magnetic field [10, 11]; the metal-insulator transition, however, still lacks adequate theoretical description.

In this paper, which summarizes results obtained in Refs. [12, 13, 14, 15, 16], we report measurements of the effective mass, m^* , and Lande g factor in a wide range of electron densities including the immediate vicinity of the MIT. We have used two independent methods to determine these parameters. In the first method, we have studied low-temperature magnetotransport in a parallel magnetic field. It turns out that the magnetic field, B_c , required to fully polarize electron spins, is a strictly linear function of the electron density: $B_c / (n_s - n_c)$ where n_c is some finite electron density close to the critical electron density n_c for the $B = 0$ metal-insulator transition. Vanishing B_c points to a sharply increasing spin susceptibility, χ / gm , and gives evidence in favour of the spontaneous spin polarization at a finite electron density. (Similar conclusion about possible spontaneous spin polarization in the dilute 2D electron system in silicon has been reached in Ref. [17].) Comparing our data for zero-field resistivity with the recent theory [10], we extract the values of m^* and g separately. It turns out that it is the value of the effective mass that becomes strongly (by more than a factor of 3) enhanced with decreasing electron density, while the g factor remains nearly constant and close to its value in bulk silicon. In the second method, we have determined the effective mass by analyzing temperature dependence of the weak-field Shubnikov-de Haas (SdH) oscillations and found good agreement with the data obtained by the first method. Furthermore, using tilted magnetic fields, we find that the value of the effective mass does not depend on the degree of spin polarization, which points to a spin-independent origin of the effective mass enhancement. This is in clear contradiction with existing theories [6, 7, 8].

2. Samples and experimental technique

Measurements have been made in a rotator-equipped Oxford dilution refrigerator with a base temperature of ≈ 30 mK on low-disordered (100)-silicon samples similar to those previously used in Ref. [18]. Peak electron mobilities in these samples are close

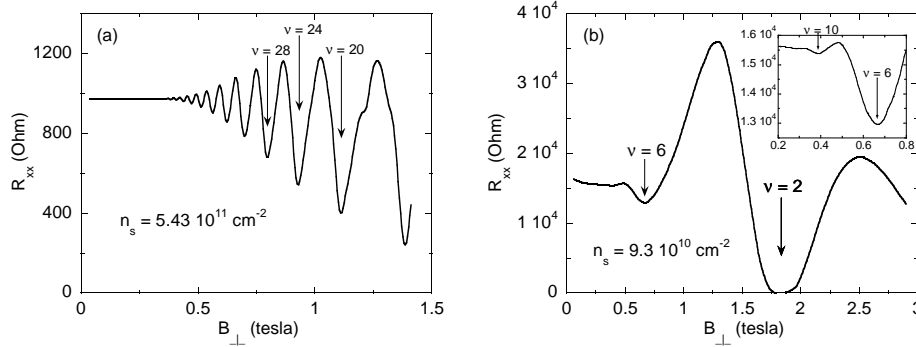


Figure 1. Shubnikov-de Haas oscillations in the Si MOSFET at $T = 40$ mK (a) at a relatively high electron density $n_s = 5.43 \cdot 10^{11} \text{ cm}^{-2}$ and (b) at low electron density $n_s = 9.3 \cdot 10^{10} \text{ cm}^{-2}$. The minima of the resistance at Landau level filling factors $\nu = 6$ and 10 are shown on an expanded scale in the inset.

to $3 \text{ m}^2/\text{Vs}$ at 0.1 K . To minimize the contact resistance, which tends to grow very high at mK temperatures and low electron density, thin gaps in the gate metallization have been introduced; this allows for maintaining high electron density near the contacts (about $1.5 \cdot 10^{12} \text{ cm}^{-2}$) regardless of its value in the main part of the sample. These gaps are narrow enough ($< 100 \text{ nm}$) for the given gate-oxide thickness to provide a smoothly descending electrostatic potential from the high-density part to the low-density part. The resistance, R_{xx} , has been measured by a standard 4-terminal technique at a low frequency (0.4 Hz) to minimize the out-of-phase signal. Excitation current has been kept low ($0.1\text{-}0.2 \text{ nA}$) to ensure that measurements are taken in the linear regime of response; the power generated in the samples has been maintained under 10^{-14} W . To verify that the electrons are not overheated, we have studied the temperature dependence of the amplitude of the SdH oscillations; the latter has been found to follow the theoretical curve down to temperatures less than 50 mK (for more on this, see below).

3. Experimental results

We start by showing a low-temperature longitudinal magnetoresistance R_{xx} in a perpendicular magnetic field B_{\perp} for a relatively high (Fig. 1(a)) and relatively low (Fig. 1(b)) electron densities. At the high density, positions of SdH oscillations correspond to "cyclotron" filling factors [19], some of which are marked by arrows. Indeed, the energy splittings $\epsilon_s = g_B B_{\perp}$ at "spin" filling factors, $\nu = 2, 6, 10, \dots = 4i - 2$, in high-density Si MOSFETs are known to be much smaller than the splittings $\epsilon_c = \hbar \omega_c = g_B B_{\perp}$ at "cyclotron" filling factors, $\nu = 4, 8, 12, \dots = 4i$, disregarding the odd valley splitting which is small (here $\omega_c = eB_{\perp}/m^*c$ is the cyclotron frequency and $i = 1, 2, 3, \dots$). The behaviour of the sample at a relatively high electron density is thus rather ordinary. In contrast, at low electron density (just above the metal-insulator transition which in this sample occurs at $n_s = n_c = 8 \cdot 10^{10} \text{ cm}^{-2}$), the magnetoresistance looks quite different [20]. The resistance minima are seen only at $\nu = 2, 6$, and 10 (see the inset); there is also a minimum at $\nu = 1$ (not shown in the figure) corresponding to the valley splitting. There are neither dips nor other anomalies at magnetic fields corresponding to $\nu = 4, 8$, or 12 where cyclotron minima

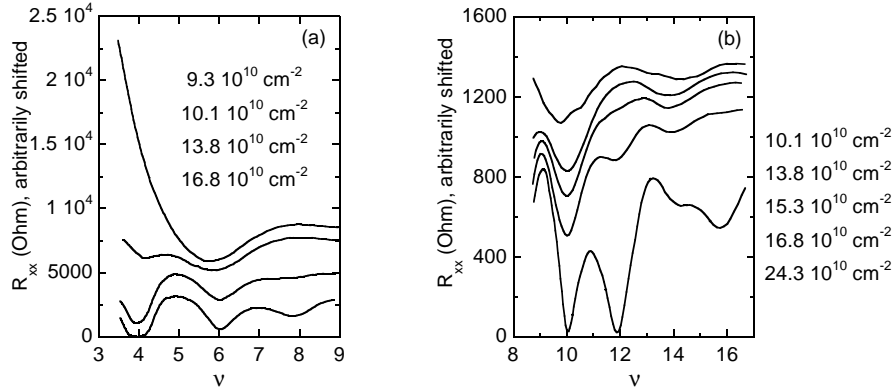


Figure 2. Evolution of the Shubnikov-de Haas oscillations with electron density in two ranges of filling factors: (a) $3 < \nu < 9$ and (b) $8 < \nu < 17$; $T = 40$ mK. The curves are vertically shifted for clarity.

are expected.

Figure 2 shows how the resistance minima corresponding to the cyclotron splittings gradually disappear as the electron density is reduced. At the highest electron densities (the lower curves), deep resistance minima near even filling factors are seen ($\nu = 4, 6,$ and 8 in Fig.2 (a); $\nu = 10, 12,$ and 16 in Fig.2 (b)), and a shallow minimum is visible at $\nu = 14$ in Fig.2 (b). As n_s is reduced, the minima at $\nu = 4, 8, 12,$ and 16 become less deep, and at the lowest electron densities (the upper curves), neither of them is seen any longer, and only minima at $\nu = 6, 10,$ and 14 remain.

Our results thus show that as one approaches the metal-insulator transition, the energy gaps at "cyclotron" filling factors become gradually smaller than those at "spin" filling factors and eventually vanish. The condition for vanishing ν_c is $g_B B_{\perp} = \hbar \omega_c$ (within the uncertainty associated with the broadening of the energy levels), or $g_B = 2m_e = 1$, which is higher by more than a factor of five than the "normal" value of this ratio, $g_B = 2m_e = 0.19$. Therefore, the spin susceptibility χ / g_B is strongly enhanced near the MIT.

One could attempt to link the observed behaviour to a many-body enhancement of spin gaps specific for a perpendicular magnetic field [21]. However, the disappearance of the cyclotron splittings in a wide range of magnetic fields would require an enhanced g -factor which is independent of magnetic field, in contradiction with Ref. [21]. On the other hand, our results are consistent with the suggestion [22] that the effective g factor is nearly field-independent and approximately equal to its many-body enhanced zero-field value. To probe this conjecture, we have studied the parallel-field magnetotransport in a wide range of electron densities.

Typical curves of the low-temperature magnetoresistance (B_{\parallel}) in a parallel magnetic field are displayed in Fig. 3. Note that the thickness of the 2D electron system in Si MOSFETs is small compared to the magnetic length in accessible fields, and, therefore, the parallel field couples largely to the electrons' spins while the orbitals are suppressed [23, 24]. The resistivity increases with field until it saturates at a constant value above a certain density-dependent magnetic field. According to Refs. [22, 25], the saturation of the magnetoresistance indicates the onset of a complete spin polarization. In the vicinity of the metal-insulator transition, the magnetoresistance is strongly T -dependent down to the lowest achievable

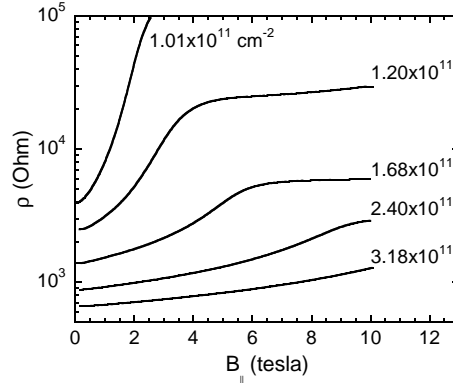


Figure 3. Low-temperature magnetoresistance in parallel magnetic fields at different electron densities above the critical density for the $B = 0$ metal-insulator transition. The lowest density curve is outside the scaling region as described in the text.

temperatures. As one moves away from the transition, however, the temperature dependences saturate at very low temperatures. The data shown below are obtained in this low-temperature limit where the magnetoresistance becomes temperature-independent.

In Fig. 4, we show how the normalized magnetoresistance, measured at different electron densities, collapses onto a single curve when plotted as a function of B_k/B_c . The scaling parameter, B_c , has been normalized to correspond to the magnetic field at which the magnetoresistance saturates (within the accuracy with which the latter can be determined). The observed scaling is remarkably good for $B_k/B_c = 0.7$ in the electron density range $1.08 \times 10^{11} - 10^{12} \text{ cm}^{-2}$, although with increasing n_s , the scaled experimental data occupy progressively shorter intervals on the resulting curve. Both at $B_k/B_c > 0.7$ and outside the indicated range of electron densities, the scaled data start to noticeably deviate from the universal curve. In particular, the scaling breaks down when one approaches ($n_s < 1.3 n_c$) the metal-insulator transition which in this sample occurs at zero magnetic field at $n_c = 8 \times 10^{10} \text{ cm}^{-2}$. This is not surprising as the magnetoresistance near n_c depends strongly on temperature, as discussed above. We note that the observed scaling dependence is described reasonably well by the theoretical dependence of $\rho(B_k/B_c)$ on the degree of spin polarization $\rho(B_k/B_c) = \rho(B_k/B_c) = h^2 n_s = B_k/B_c$ predicted by the recent theory [26].

In Fig. 5, B_c is plotted vs. n_s . With high accuracy, B_c is proportional to the deviation of the electron density from its critical value, i.e., to $(n_s - n_c)$, over a wide range of electron densities. In other words, the field, at which the magnetoresistance saturates, tends to vanish at n_c (see also Refs. [15, 27]). We emphasize that our procedure provides high accuracy for determining the behaviour of the field of saturation with electron density, i.e., the functional form of $B_c(n_s)$, even though the absolute value of B_c is determined not so accurately. Note that at n_s above $2.4 \times 10^{11} \text{ cm}^{-2}$, the saturation of the resistance is not reached in our magnetic field range; still, the high precision of the collapse of the high-density experimental curves onto the same scaling curve as the low-density data allows us to draw conclusions about the validity of the obtained law $B_c(n_s)$ over a much wider range of electron densities.

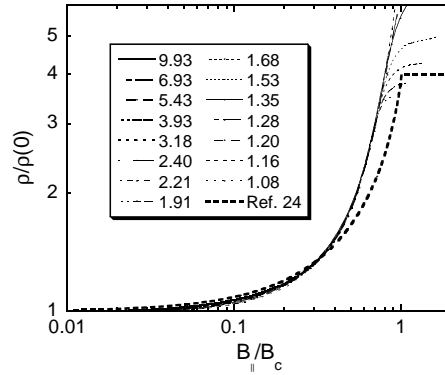


Figure 4. Scaled curves of the normalized magnetoresistance at different n_s vs. B/B_c . The electron densities are indicated in units of 10^{11} cm^{-2} . Also shown by a dashed line is the normalized magnetoresistance calculated in Ref. [26].

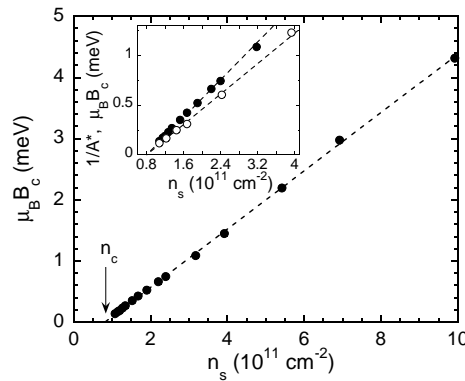


Figure 5. Dependence of the field B_c on electron density. The dashed line is a linear fit which extrapolates to the critical electron density for the $B = 0$ metal-insulator transition. Comparison of $1/A^*(n_s)$ (see Eq. (1)) and $B_c(n_s)$ (open and solid circles, correspondingly) is shown in the inset. The dashed lines are linear fits which extrapolate to the critical electron density for the metal-insulator transition.

The observed tendency of B_c to vanish at a finite electron density is consistent with the strong increase of the spin susceptibility χ/gm [12, 15, 28] and gives evidence in favour of a spontaneous spin polarization at $n = n_c$. In principle, either g or m (or both) may be responsible for the strong increase of the spin susceptibility. As has already been mentioned, within the Fermi liquid theory, both the effective mass and g factor are renormalized due to spin exchange effects, with renormalization of the g factor being dominant compared to that of the effective mass. In contrast, the dominant increase of the effective mass follows from an alternative description of the strongly-interacting electron system beyond the Fermi liquid approach [7, 8]. To separate g and m , we have measured the temperature-dependent conductivity in zero magnetic field and analyzed the data in the spirit of recent theory [10]. According to

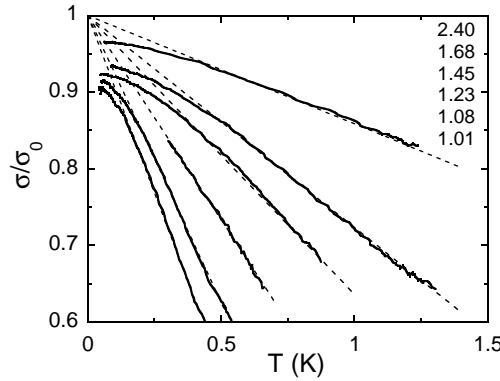


Figure 6. The temperature dependence of the normalized conductivity at different electron densities (indicated in units of 10^{11}cm^{-2}) above the critical electron density for the metal-insulator transition. The dashed lines are fits of the linear interval of the dependence.

this theory, $\sigma(T)$ is a linear function of temperature:

$$\frac{\sigma(T)}{\sigma_0} = 1 - A k_B T; \tag{1}$$

where the slope, A , is determined by the interaction-related parameters: the Fermi liquid constants, F_0^a and F_1^s :

$$A = \frac{(1 + F_0^a) g m}{h^2 n_s}; \tag{2}$$

The factor g is equal to 8 in our case [29]. This theoretical relation allows us to determine the many-body enhanced g factor and mass m separately using the data for the slope A and the product $g m$.

Typical dependences of the normalized conductivity on temperature, $\sigma(T)/\sigma_0$, are displayed in Fig. 6 at different electron densities above n_c ; the value σ_0 , which has been used to normalize σ , was obtained by extrapolating the linear interval of the $\sigma(T)$ dependence to $T = 0$. As long as the deviation $j = \sigma_0 - \sigma$ is sufficiently small, the conductivity increases linearly with decreasing T in agreement with Eq. (1), until it saturates at the lowest temperatures. As seen from the figure, the linear interval of the dependence is wide enough to make a reliable fit.

The n_s dependence of the inverse slope $1/A$, extracted from the $\sigma(T)$ data, is shown in the inset to Fig. 5 by open circles. Over a wide range of electron densities, the values $1/A$ and B_c turn out to be close to each other. The low-density data for $1/A$ are approximated well by a linear dependence which extrapolates to the critical electron density n_c in a similar way to the behaviour of the polarization field B_c .

In Fig. 7, we show the so-determined values $g = g_0$ and $m = m_b$ as a function of the electron density (here $g_0 = 2$ is the g factor in bulk silicon, m_b is the band mass equal to $0.19 m_e$, and m_e is the free electron mass). In the high n_s region (relatively weak interactions), the enhancement of both g and m is relatively small, both values slightly increasing with decreasing electron density in agreement with earlier data [30]. Also, the renormalization of the g factor is dominant compared to that of the effective mass, which is consistent with theoretical studies [6].

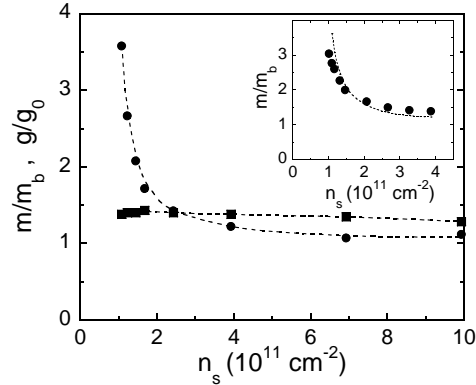


Figure 7. The effective mass (circles) and g factor (squares), determined from the analysis of the parallel field magnetoresistance and temperature-dependent conductivity, vs. electron density. The dashed lines are guides to the eye. The inset compares the so-obtained effective mass (dotted line) with the one extracted from the analysis of SdH oscillations (circles).

In contrast, the renormalization at low n_s (near the critical region), where $r_s \gg 1$, is much more striking. As the electron density is decreased, the renormalization of the effective mass overshoots abruptly while that of the g factor remains relatively small, $g \approx g_0$, without tending to increase. Hence, the current analysis indicates that it is the effective mass, rather than the g factor, that is responsible for the drastically enhanced gm value near the metal-insulator transition.

Since the procedure for extracting g and m described above relies on theoretically calculated functional form for the slope A [10], we have performed independent measurements of the effective mass based on the temperature analysis of the amplitude, A , of the weak-field (sinusoidal) SdH oscillations. A typical temperature dependence of A for the normalized resistance, $R_{xx} = R_0$ (where R_0 is the average resistance), is displayed in Fig. 8. To determine the effective mass, we use the method of Ref. [31] extending it to much lower electron densities and temperatures. We fit the data for $A(T)$ using the formula

$$A(T) = A \frac{2^2 k_B T = \hbar c}{\sinh(2^2 k_B T = \hbar c)}; \text{ where } A = 4 \exp(-2^2 k_B T_D = \hbar c); \quad (3)$$

where T_D is the Dingle temperature. As the latter is related to the level width through the expression $T_D = \hbar / 2 k_B \tau$ (where τ is the elastic scattering time) [10], damping of the SdH oscillations with temperature may be influenced by temperature-dependent τ . We have verified that in the studied low-temperature limit for electron densities down to $1 \times 10^{11} \text{ cm}^{-2}$, possible corrections to the mass value caused by the temperature dependence of τ (and hence T_D) are within our experimental uncertainty which is estimated at about 10%. Note that the amplitude of the SdH oscillations follows the calculated curve down to the lowest achieved temperatures, which confirms that the electrons were in a good thermal contact with the bath and were not overheated. The fact that the experimental dependence $A(T)$ follows the theoretical curve justifies applicability of Eq. (3) to this strongly-interacting electron system.

The so-determined effective mass is shown in the inset to Fig. 7. In quantitative agreement with the results obtained by the alternative method described above (the

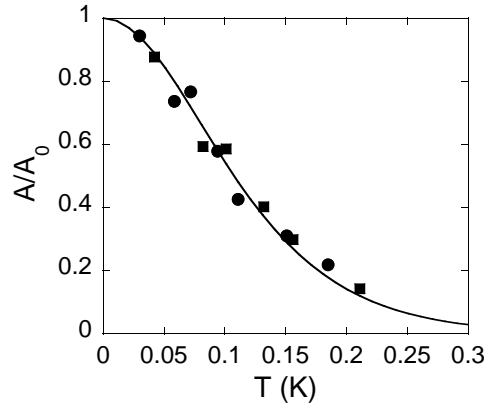


Figure 8. Amplitude of the weak-field SdH oscillations vs. temperature at $n_s = 1.17 \times 10^{11} \text{ cm}^{-2}$ for oscillation numbers $\nu = \hbar c n_s / e B_{\perp} = 10$ (dots) and $\nu = 14$ (squares). The value of T for the $\nu = 10$ data is divided by the factor of 1.4. The solid line is a fit using Eq. (3).

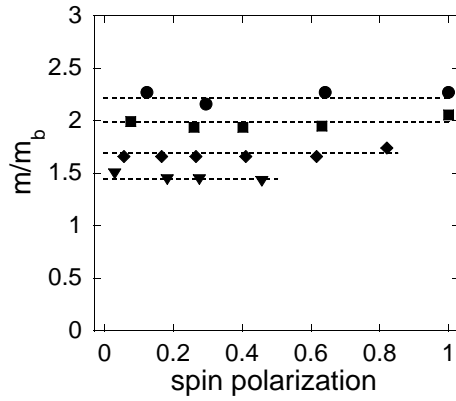


Figure 9. The effective mass vs. the degree of spin polarization for the following electron densities in units of 10^{11} cm^{-2} : 1.32 (dots), 1.47 (squares), 2.07 (diamonds), and 2.67 (triangles). The dashed lines are guides to the eye.

dotted line), the effective mass sharply increases with decreasing n_s . The agreement between the results obtained by two independent methods adds confidence in our results and conclusions. Our data are also consistent with the data for spin and cyclotron gaps obtained by magnetocapacitance spectroscopy [32].

A strong enhancement of m at low electron densities may originate from spin effects [6, 7, 8]. With the aim of probing a possible contribution from the spin effects, we have introduced a parallel magnetic field component to align the electrons' spins. In Fig. 9, we show the behaviour of the effective mass with the degree of spin polarization, $p = (B_{\perp}^2 + B_{\parallel}^2)^{1/2} / B_c$. As seen from the figure, within our accuracy, the effective mass m does not depend on p . Therefore, the $m(n_s)$ dependence is robust, the origin of the mass enhancement has no relation to the electrons' spins and exchange effects [33].

4. Discussion

Under the conditions of our experiments, the interaction parameter, r_s , is larger by a factor of $2m^*/m_b$ than the Wigner-Seitz radius and reaches approximately 50, which is above the theoretical estimate for the onset of Wigner crystallization. As has already been mentioned, two approaches to calculate the renormalization of m^* and g have been formulated. The first one exploits the Fermi liquid model extending it to relatively large r_s . Its main outcome is that the renormalization of g is large compared to that of m^* [6]. In the limiting case of high r_s , one may expect a divergence of the g factor that corresponds to the Stoner instability. These predictions are in obvious contradiction to our data: (i) the behaviour of the 2D dilute system in the regime of the strongly enhanced susceptibility close to the onset of spontaneous spin polarization and Wigner crystallization is governed by the effective mass, rather than the g factor, through the interaction parameter r_s ; and (ii) the insensitivity of the effective mass to spin effects also cannot be accounted for.

The other theoretical approach either employs analogy between a strongly interacting 2D electron system and He^3 [7] or applies Gutzwiller's variational method [35] to Si MOSFETs [8]. It predicts that near the crystallization point, the renormalization of m^* is dominant compared to that of g and that the effective mass tends to diverge at the transition. Although the sharp increase of the mass is in agreement with our findings, it is the expected dependence of m^* on the degree of spin polarization that is not confirmed by our data: the model of Ref. [7] predicts that the effective mass should increase with increasing spin polarization, whereas the prediction of the other model [8] is the opposite.

Thus, the existing theories fail to explain our finding that in a dilute 2D electron system the effective mass is strongly enhanced and does not depend on the degree of spin polarization. The fact that the spin exchange is not responsible for the observed mass enhancement reduces the chances for the occurrence of the ferromagnetic Fermi liquid prior to the Wigner crystallization. However, should the spin exchange be small, the spin effects may still come into play closer to the onset of Wigner crystallization where the Fermi energy may continue dropping as caused by mass enhancement.

In summary, we have found that in very dilute two-dimensional electron systems in silicon, the effective mass sharply increases with decreasing electron density, while the g factor remains nearly constant and close to its value in bulk silicon. The enhanced effective mass does not depend on the degree of the spin polarization and, therefore, its increase is not related to spin exchange effects, in contradiction with existing theories. The corresponding strong rise of the spin susceptibility may be a precursor of a spontaneous spin polarization; unlike in the Stoner scenario, the latter originates from the enhancement of the effective mass rather than the increase of the g factor. Our results show that the dilute 2D electron system in silicon behaves well beyond the weakly interacting Fermi liquid.

Acknowledgments

We gratefully acknowledge discussions with I. L. Aleiner, D. Heinan, F. Kusmartsev, M. P. Sarachik, B. Spivak, and S. A. Vitkalov. This work was supported by the National Science Foundation grants DMR-9988283 and DMR-0129652, the Sloan Foundation, the Russian Foundation for Basic Research, the Russian Ministry of Sciences, and the Program "The State Support of Leading Scientific Schools".

References

- [1] E. Wigner, Phys. Rev. 46, 1002 (1934).
- [2] E. C. Stoner, Rept. Prog. Phys. 11, 43 (1947).
- [3] L. D. Landau, Sov. Phys. JETP 3, 920 (1957).
- [4] B. Tanatar and D. M. Ceperley, Phys. Rev. B 39, 5005 (1989).
- [5] C. Attaccalite, S. Moroni, P. Gorio, and G. B. Bachelet, Phys. Rev. Lett. 88, 256601 (2002).
- [6] N. Iwamoto, Phys. Rev. B 43, 2174 (1991); Y. Kwon, D. M. Ceperley, and R. M. Martin, *ibid.* 50, 1684 (1994); G.-H. Chen and M. E. Raikh, *ibid.* 60, 4826 (1999).
- [7] B. Spivak, Phys. Rev. B 64, 085317 (2001).
- [8] V. T. Dolgoplov, JETP Lett. 76, 377 (2002).
- [9] E. Abraham, S. V. K ravchenko, and M. P. Sarachik, Rev. Mod. Phys. 73, 251 (2001).
- [10] G. Zala, B. N. Narozhny, and I. L. Aleiner, Phys. Rev. B 64, 214204 (2001).
- [11] A. Punnoose and A. M. Finkelstein, Phys. Rev. Lett. 88, 016802 (2002).
- [12] S. V. K ravchenko, A. A. Shashkin, D. A. Bore, and T. M. K lapwijk, Solid State Comm. 116, 495 (2000).
- [13] A. A. Shashkin, S. V. K ravchenko, V. T. Dolgoplov, and T. M. K lapwijk, Phys. Rev. Lett. 87, 086801 (2001).
- [14] A. A. Shashkin, S. V. K ravchenko, V. T. Dolgoplov, and T. M. K lapwijk, Phys. Rev. B 66, 073303 (2002).
- [15] S. V. K ravchenko, A. A. Shashkin, and V. T. Dolgoplov, Phys. Rev. Lett. 89, 219701 (2002).
- [16] A. A. Shashkin, M. Rahimi, S. Anisimova, S. V. K ravchenko, V. T. Dolgoplov, and T. M. K lapwijk, preprint cond-mat/0301187.
- [17] S. A. Vitkalov, H. Zheng, K. M. Mertes, M. P. Sarachik, and T. M. K lapwijk, Phys. Rev. Lett. 87, 086401 (2001).
- [18] R. Heemskerk and T. M. K lapwijk, Phys. Rev. B 58, R1754 (1998).
- [19] In silicon MOSFETs, "cyclotron" gaps correspond to $\nu = 4, 8, 12, 16, \dots$ while "spin" gaps correspond to $\nu = 2, 6, 10, 14, \dots$ due to a two-fold valley degeneracy in this system.
- [20] This unusual behaviour was first reported by M. D'Orto, V. M. Pudalov, and S. G. Semenchinsky, Phys. Lett. A 150, 422 (1990).
- [21] Yu. A. Bychkov, S. V. Iordanskii, and G. M. Eliashberg, JETP Lett. 33, 143 (1981); C. Kallin and B. I. Halperin, Phys. Rev. B 30, 5655 (1984); A. H. MacDonald, H. C. Ojji, and K. L. Liu, Phys. Rev. B 34, 2681 (1986).
- [22] T. Okamoto, K. Hosoya, S. Kawaji, and A. Yagi, Phys. Rev. Lett. 82, 3875 (1999).
- [23] D. Simoni, S. V. K ravchenko, M. P. Sarachik, and V. M. Pudalov, Phys. Rev. Lett. 79, 2304 (1997).
- [24] The case for the 2D carrier system in GaAs is opposite to that for Si, because the orbitals in GaAs give rise to an enhancement of the effective mass in parallel magnetic fields, see, e.g., E. Tutuc et al., cond-mat/0301027.
- [25] S. A. Vitkalov, H. Zheng, K. M. Mertes, M. P. Sarachik, and T. M. K lapwijk, Phys. Rev. Lett. 85, 2164 (2000).
- [26] V. T. Dolgoplov and A. Gold, JETP Lett. 71, 27 (2000).
- [27] S. A. Vitkalov, M. P. Sarachik, and T. M. K lapwijk, Phys. Rev. B 65, 201106(R) (2002).
- [28] V. M. Pudalov, M. E. Gershenson, H. Kojima, N. Butch, E. M. Dzhur, G. Brunthaler, A. Prinz, and G. Bauer, Phys. Rev. Lett. 88, 196404 (2002).
- [29] I. L. Aleiner, private communication. For low intervalley scattering, $\nu = 8$ if $T < \nu$ and $\nu = 16$ if $T > \nu$, where ν is the valley splitting. Both experimental (see, e.g., V. M. Pudalov, A. Punnoose, G. Brunthaler, A. Prinz, and G. Bauer, cond-mat/0104347) and theoretical (see Ref. [30]) studies give an estimate for $\nu \approx 1.5 K$.
- [30] T. Ando, A. B. Fowler, and F. Stem, Rev. Mod. Phys. 54, 437 (1982).
- [31] J. L. Smith and P. J. Stiles, Phys. Rev. Lett. 29, 102 (1972).
- [32] V. S. Khrapai, A. A. Shashkin, and V. T. Dolgoplov, cond-mat/0301361.
- [33] In principle, the exchange effects can also originate from the isospin degree of freedom in bivalley (100)-Si MOSFETs. The valley origin of the strongly enhanced effective mass is not very likely, as inferred from a similar increase of the ratio of the spin and the cyclotron splittings at low n_s in the 2D electron system in GaAs [34].
- [34] J. Zhu, H. L. Stormer, L. N. Pfeiffer, K. W. Baldwin, and K. W. West, Phys. Rev. Lett. (2003, in press).
- [35] W. F. Brinkman and T. M. Rice, Phys. Rev. B 2, 4302 (1970).